

# Transverse negative magnetoresistance of 2D structures in the presence of strong in-plane magnetic field: weak localization as a probe of interface roughness

G. M. Minkov,<sup>\*</sup> O. E. Rut, A. V. Germanenko, and A. A. Sherstobitov

*Institute of Physics and Applied Mathematics,  
Ural State University, 620083 Ekaterinburg, Russia*

B. N. Zvonkov

*Physical-Technical Research Institute,  
University of Nizhni Novgorod, Nizhni Novgorod 603600, Russia*

D. O. Filatov

*Research and Educational Center for Physics of the Solid State Nanostructures,  
University of Nizhny Novgorod, Nizhni Novgorod 603600, Russia*

(Dated: November 9, 2018)

## Abstract

The interference induced transverse negative magnetoresistance of GaAs/In<sub>x</sub>Ga<sub>1-x</sub>As/GaAs quantum well heterostructures has been studied in the presence of strong in-plane magnetic field. It is shown that effect of in-plane magnetic field is determined by the interface roughness and strongly depends on the relationship between mean free path, phase breaking length and roughness correlation length. Analysis of the experimental results allows us to estimate parameters of short- and long-range correlated roughness which have been found in a good agreement with atomic force microscopy data obtained for just the same samples.

PACS numbers: 73.20.Fz, 73.61.Ey

## I. INTRODUCTION

The interference correction determines in the main the temperature and magnetic field dependences of the conductivity of weakly disordered two-dimensional (2D) systems. This correction originates in the constructive interference of time-reversed electron trajectories. For an ideal two-dimensional gas of spin-less particles only perpendicular magnetic field  $B_{\perp}$  destroys the interference resulting in negative magnetoresistance, whereas an in-plane magnetic field  $B_{\parallel}$  does not effect the interference correction.<sup>1</sup> Therefore, an applying of in-plane magnetic field should not change the magnetoresistance caused by the perpendicular field.

For real 2D system placed in in-plane magnetic field an interface roughness leads to that an electron effectively feels random perpendicular magnetic field at motion. This effect not only gives rise to the negative magnetoresistance at in-plane magnetic field but changes the magnetoresistance in perpendicular field in the presence of in-plane field.

Another mechanism of influence of in-plane magnetic field on the interference correction is the spin relaxation. If the relaxation is strong enough it suppresses the weak localization leading to positive magnetoresistance in very low magnetic field and appearance of so-called antilocalization maximum on the resistivity-magnetic field curve. In-plane magnetic field resulting in Zeeman splitting decreases the spin relaxation rate and, thus, affects the interference induced magnetoresistance.<sup>2</sup> This mechanism is not effective in considerably dirty systems, in which the spin-relaxation rate is less than the dephasing rate and antilocalization maximum is not evident even at very low temperature.

Anomalous low field magnetoresistance at perpendicular magnetic field has been studied extensively for many years. Considerably less attention has been directed to the effect of in-plane magnetic field on interference correction. Although the effects are small they are interesting because give an information on interface roughness of 2D structures. The first detailed experimental study of effects of in-plane magnetic field on negative magnetoresistance at perpendicular field was carried out in Ref. 3 for silicon MOSFETs. There was shown that short-range correlated roughness ( $L < l_p$ , where  $L$  is distance over which fluctuations are correlated and  $l_p$  is mean free path) leads to decreasing of phase breaking time ( $\tau_{\varphi}$ ) by in-plane magnetic field and thus to changing of the shape of magnetoresistance curve. The theoretical analysis carried out in recent paper by Mathur and Baranger<sup>4</sup> shows that

effect of in-plane magnetic field on the shape of magnetoresistance curve strongly depends on relationship between  $L$ ,  $l_p$  and  $l_\varphi = \sqrt{D\tau_\varphi}$ , where  $D$  is diffusion coefficient. Thus, the experimental studies of the interference correction in the presence of in-plane magnetic field gives a possibility to find the parameters of interface roughness in particular structure.

This paper is devoted to the experimental study of the interference induced transverse negative magnetoresistance of GaAs/In<sub>x</sub>Ga<sub>1-x</sub>As/GaAs quantum wells with different scales of interface roughness in the presence of strong in-plane magnetic field. It is organized as follows. In the next section we give experimental details. Experimental results are presented and discussed in Sec. III: Sec. III A and Sec. III B are dedicated to results of magnetoresistance measurements for the samples with short- and long-correlated roughness, respectively, Sec. III C is concerned with the results of atomic force microscopy.

## II. EXPERIMENTAL DETAILS

In the present work we experimentally study the two types of single quantum well heterostructures. The structure 3512 is GaAs/InGaAs/GaAs quantum well heterostructure which consists of 0.5  $\mu\text{m}$ -thick undoped GaAs epilayer, a Sn  $\delta$ -layer, a 9 nm spacer of undoped GaAs, a 8 nm In<sub>0.2</sub>Ga<sub>0.8</sub>As well, a 9 nm spacer of undoped GaAs, a Sn  $\delta$ -layer, and a 300 nm cap layer of undoped GaAs. In the second structure, H5610, the arrangement of the doped layers was the same as in the first one. The difference only is that the thin layer of InAs instead of In<sub>0.2</sub>Ga<sub>0.8</sub>As layer has been grown. The large lattice mismatch between InAs and GaAs results in this case in formation of nanoclusters. They are situated on the InAs wetting layer of one-two monolayers thickness, which is thin deep quantum well for electrons. The samples were mesa etched into standard Hall bars and then an Al gate electrode was deposited by thermal evaporation onto the cap layer through a mask. Applying the gate voltage  $V_g$  we were able to change the electron density and conductivity of 2D gas. At electron density higher than approximately  $7 \times 10^{11} \text{ cm}^{-2}$  for structure 3512 and  $9 \times 10^{11} \text{ cm}^{-2}$  for structure H5610, the states in  $\delta$ -layers start to be occupied that affects the dephasing rate and influences the magnetoresistance curve.<sup>5</sup> In the present paper we restrict our consideration by the case when the states in  $\delta$ -layers are empty. In opposite case additional effects in parallel magnetic field occur which will be considered elsewhere. The structures parameters for some gate voltage are presented in Table I.

TABLE I: The parameters for the structures for different gate voltages

Structure	$V_g$ (V)	$n(10^{12} \text{ cm}^{-2})$	$\sigma(G_0)^a$	$\sigma_0(G_0)^b$	$\tau_p(10^{-13} \text{ s})$	$B_{tr}(\text{T})$
3512	0.0	1.0	165.08	169.5	4.4	0.0071
	-0.5	0.88	122.95	127.6	3.8	0.011
	-0.75	0.69	83.61	88.7	3.4	0.018
	-1.0	0.67	70.4	75.5	3.0	0.024
	-1.5	0.47	20.35	26.4	1.47	0.138
	-2.5	0.32	4.27	9.3	0.76	0.76
5610#1 <sup>c</sup>	-1.0	0.91	38.8	45.3	1.31	0.091
	-2.5	0.73	22.96	29.5	1.06	0.172
	-3.5	0.59	10.27	16.4	0.73	0.45

<sup>a</sup>Measured at T=1.45 K

<sup>b</sup>The value of the Drude conductivity has been obtained as described in Ref. 6

<sup>c</sup>The parameters of the sample #2 were analogous

In order to apply tesla-scale in-plane magnetic field while sweeping subgauss control of perpendicular field, we mount the sample with 2D electrons aligned to the axis of primary solenoid (accurate to  $\sim 1^\circ$ ) and use an independent split-coil solenoid to provide  $B_\perp$  as well as to compensate for sample misalignment. The two calibrated Hall probes were used to measure  $B_\perp$  and  $B_\parallel$ .

### III. RESULTS AND DISCUSSION

To make evident the difference in the effect of in-plane magnetic field on the shape of negative magnetoresistance at perpendicular field for these structures we have presented the data for both structures in Fig. 1 together. The magnetic field scale has been normalized to characteristic for weak localization field  $B_{tr} = \hbar/(2el_p^2)$ . One can see that in-plane magnetic field changes the shape of magnetoresistance curve within wide range of perpendicular field for structure 3512, while for structure H5610 the changes of the shape occur at low perpendicular field only. Below we demonstrate that this difference results from the different correlation lengths of roughness in these structures.

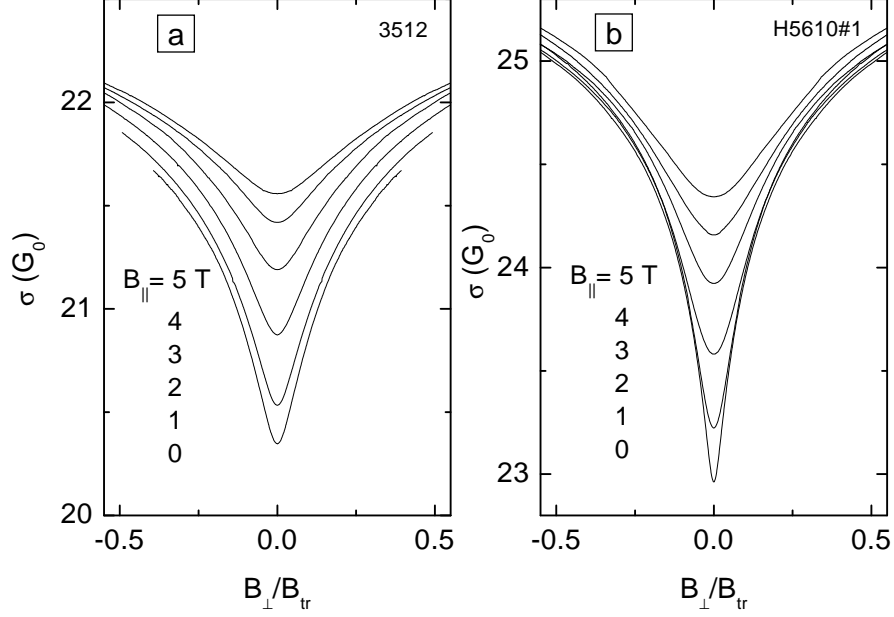


FIG. 1: The conductivity  $\sigma$  as a function of  $B_{\perp}$  dependences measured at  $T = 1.45$  K for different in-plane magnetic fields for structure 3512,  $V_g = -1.5$  V (a) and structure H5610#1,  $V_g = -2.5$  V (b).

### A. The role of short-range correlated roughness

Firstly, let us consider the data for the structure 3512. Thorough studying of the weak localization correction at  $B_{\parallel} = 0$  shows that experimental data are in excellent agreement with conventional theory:

1. Magnetoconductance is well described by standard Hikami-Larkin-Nagaoka (HLN) expression<sup>7</sup>

$$\begin{aligned} \Delta\sigma(B) &= \rho_{xx}^{-1}(B) - \rho_{xx}^{-1}(0) = \alpha G_0 H(B, \tau_{\varphi}), \\ H(B, \tau_{\varphi}) &\equiv \psi\left(\frac{1}{2} + \frac{\tau_p B_{tr}}{\tau_{\varphi} B}\right) - \psi\left(\frac{1}{2} + \frac{B_{tr}}{B}\right) - \ln\left(\frac{\tau_p}{\tau_{\varphi}}\right) \end{aligned} \quad (1)$$

with  $\alpha$  and  $\tau_{\varphi}$  as fitting parameters. In Eq. (1),  $G_0 = e^2/(2\pi^2\hbar)$ ,  $\psi(x)$  is a digamma function,  $\tau_{\varphi}$  is the phase breaking time. For strictly diffusion regime ( $\tau_p/\tau_{\varphi} \ll 1$ ,  $B/B_{tr} \ll 1$ ) the prefactor  $\alpha$  has to be equal to unity. As Fig. 2(a) illustrates, the values of the fitting parameters  $\alpha$  and  $\tau_{\varphi}$  only slightly depend on the magnetic field interval in which the fit is done.

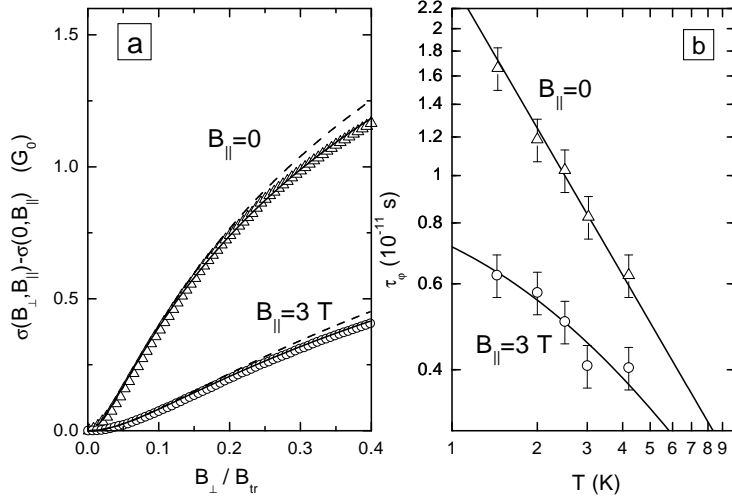


FIG. 2: (a) The  $[\sigma(B_{\perp}, B_{\parallel}) - \sigma(0, B_{\parallel})]$ -versus- $B_{\perp}$  dependences for structure 3512 at  $B_{\parallel} = 0$  and 3 T,  $T = 1.45$  K,  $V_g = -1$  V. Symbols are the experimental data. Curves are the best fit by Eq. (1) with parameters:  $B_{\parallel} = 0$  –  $\alpha = 0.98$  and  $\tau_{\phi} = 1.5 \times 10^{-11}$  s (dashed curve),  $\alpha = 0.87$  and  $\tau_{\phi} = 1.65 \times 10^{-11}$  s (solid curve);  $B_{\parallel} = 3$  T –  $\alpha = 0.75$  and  $\tau_{\phi}^* = 0.56 \times 10^{-11}$  s (dashed curve),  $\alpha = 0.62$  and  $\tau_{\phi}^* = 0.63 \times 10^{-11}$  s (solid curve). Dashed and solid curves correspond to the fitting interval  $B = (0 - 0.1)B_{tr}$  and  $B = (0 - 0.2)B_{tr}$ , respectively. (b) The temperature dependence of the dephasing time for  $B_{\parallel} = 0$  and 3 T for structure 3512. Symbols are the experimental data. Upper line is  $T^{-1}$ -law, lower one is drawn as described in the text.

2. The temperature dependence of  $\tau_{\phi}$  is close to  $T^{-1}$ -law [see Fig. 2(b)].
3. The temperature dependence of the conductivity at  $B = 0$  is logarithmic. Slope of the experimental  $\sigma/G_0$ -versus- $\ln T$  dependence is about  $1.45 \pm 0.05$ . Here, the unity comes from the weak localization and 0.45 comes from the electron-electron interaction.<sup>6</sup>

Now let us analyze the data when in-plane magnetic field is applied. As seen from Fig. 2(a) in this case the magnetoconductance  $\sigma(B_{\perp}, B_{\parallel}) - \sigma(0, B_{\parallel})$  is well described by Eq. (1) also and the fitting parameters  $\alpha$  and  $\tau_{\phi}^*$  (hereinafter,  $\tau_{\phi}$  relating to  $B_{\parallel} \neq 0$  will be labelled as  $\tau_{\phi}^*$ ) depends only slightly on the fitting interval. As clearly seen from Fig. 3(a) the value of  $\tau_{\phi}^*$  strongly decreases when  $B_{\parallel}$  increases.

The effect of in-plane magnetic field on the negative magnetoresistance can be understood as follows. The weak localization correction to the conductivity results from the interference of electron waves scattered along closed trajectories in opposite directions (time-

reversed paths). Magnetic field gives the phase difference between pairs of time-reversed paths  $\varphi = 2\pi\mathbf{BS}/\Phi_0$  (where  $\Phi_0$  is the quantum of magnetic flux,  $\mathbf{S}$  is the algebraic area enclosed) and thus destroys the interference and results in negative magnetoresistance. The scalar product  $\mathbf{BS}$  is zero for ideal 2D structures at in-plane magnetic field therefore this field does not destroy the interference, and the negative magnetoresistance is absent in this magnetic field orientation. In real 2D structure the mean electron position in growth direction randomly changes at motion along closed paths due to interface roughness. Therefore the product  $\mathbf{BS}$  becomes nonzero for in-plane magnetic field that leads to suppression of the weak localization correction. Theoretical analysis<sup>3,4,8</sup> shows that for the case of short-range correlated roughness the role of in-plane magnetic field reduces to increasing of the dephasing rate

$$\frac{1}{\tau_\varphi^*} = \frac{1}{\tau_\varphi} + \frac{1}{\tau_\parallel} \quad (2)$$

where  $\tau_\parallel^{-1}$  is determined by parameters of roughness<sup>4</sup>

$$\frac{1}{\tau_\parallel} \simeq \frac{1}{\tau_p} \frac{\sqrt{\pi}}{4} \frac{\Delta^2 L}{l_p^3} \left( \frac{B_\parallel}{B_{tr}} \right)^2. \quad (3)$$

Here,  $\Delta$  is the root-mean-square height of the fluctuations, and  $L$  is the distance over which the fluctuations are correlated.

Let us consider how our experimental results for structure 3512 agree with this model. Fig. 3(a) shows that  $\tau_p/\tau_\varphi^*$  increases linearly with  $B_\parallel^2$  in a full agreement with Eqs. (2) and (3), therewith the slope of this dependence is temperature independent. In framework of this model the temperature dependence of  $\tau_\varphi^*$  at the presence of in-plane magnetic field has to saturate on the value  $\tau_\parallel$  with decreasing temperature. Figure 2(b) in which the experimental results obtained for  $B_\parallel = 3$  T are plotted shows that  $\tau_\varphi^*$ -versus- $T$  dependence really tends to saturate at  $T \rightarrow 0$ . In the same figure we plot the  $\tau_\varphi^*$ -versus- $T$  curve calculated in accordance with Eq. (2). In this calculation the dependence  $2.5 \times 10^{-11}/T$  which is a good interpolation of experimental data for  $B_\parallel = 0$  [see Fig. 2(b)] has been used as  $\tau_\varphi(T)$  in right-hand side of Eq. (2). The quantity  $\tau_\parallel^{-1} = 1 \times 10^{11} \text{ s}^{-1}$  has been obtained as a difference between two values  $(\tau_\varphi^*)^{-1}$  and  $\tau_\varphi^{-1}$  found experimentally at  $T = 1.45$  K. Good agreement is evident within whole temperature range.

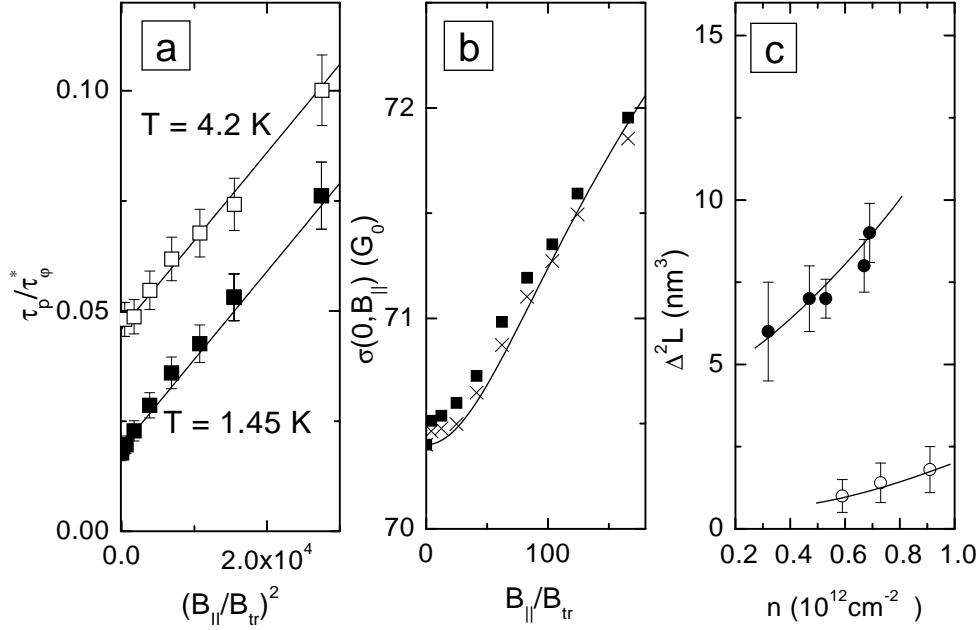


FIG. 3: (a) The value of  $\tau_p/\tau_\phi^*$  as a function of  $B_{||}^2$  for structure 3512 at  $T = 1.45$  and  $4.2$  K,  $V_g = -1$  V. Symbols are experimental results. Lines are calculated from Eqs. (2) and (3) using  $\Delta^2 L = 7.2 \text{ nm}^3$ ,  $l_p = 117 \text{ nm}$ ,  $\tau_p/\tau_\phi = 0.018$  ( $T = 1.45 \text{ K}$ ) and  $0.048$  ( $T = 4.2 \text{ K}$ ). (b) The conductivity as a function of in-plane magnetic field for structure 3512,  $T = 1.45$ ,  $V_g = -1$  V. Squares are direct experimental measurements. Crosses are obtained as  $\sigma(B_{||}) = \sigma(B_{||} = 0) + \ln(\tau_\phi/\tau_\phi^*)$ , where  $\tau_\phi$  and  $\tau_\phi^*$  have been obtained from the fit of experimental curve  $\Delta\sigma(B_\perp)$  at  $B_{||} = 0$  and  $B_{||} \neq 0$ , respectively. Solid line is Eq. (4b) with  $\Delta^2 L = 7.2 \text{ nm}^3$  and  $l_p = 117 \text{ nm}$ . (c) The electron density dependence of the parameter  $\Delta^2 L$  for structures 3512 (solid symbols) and H5610 (open symbols). Lines are provided as a guide to the eye.

This model predicts also that growth of in-plane magnetic field has to lead to increase of conductivity at  $B_\perp = 0$  as follows

$$\sigma(0, B_{||}) = \sigma(0, 0) + G_0 \ln \frac{\tau_\phi}{\tau_\phi^*} \quad (4a)$$

$$\simeq \sigma(0, 0) + G_0 \ln \left[ 1 + \frac{\tau_\phi}{\tau_p} \frac{\sqrt{\pi}}{4} \frac{\Delta^2 L}{l_p^3} \left( \frac{B_{||}}{B_{tr}} \right)^2 \right]. \quad (4b)$$

In Fig. 3(c) we present the in-plane magnetic field dependence of the conductivity which was measured directly and was calculated from Eq. (4a) using  $\tau_\phi^*$  found above [see Fig. 3(a)]. One can see that within experimental error these data agree each other satisfactorily. Thus, all effects predicted for the case of the short-range correlated roughness are observed in the



structure 3512. Therefore we believe that the slope of  $\tau_p/\tau_\phi^*$ -versus- $(B/B_{tr})^2$  dependence gives the parameter of roughness  $\Delta^2 L$  which with the use of  $l_p = 117$  nm for  $V_g = -1$  V can be estimated as  $\Delta^2 L \simeq 7.2$  nm<sup>3</sup>. Naturally, Eq. (4b) with this value of  $\Delta^2 L$  well describes the experimental in-plane magnetic field dependences of the conductivity, measured without perpendicular magnetic field [Fig. 3(b)].

We have carried out such analysis for various gate voltages and plotted the electron density dependence of  $\Delta^2 L$  in Fig. 3(c). One can see that the value of  $\Delta^2 L$  somewhat decreases with decreasing electron density. The following model can explain this observation. The inner interface lying in the depth of the structure has smaller roughness than that lying closer to the cap layer. With the decrease of the gate voltage, i.e., with decrease of the electron density, the wave function is hold closer against the inner interface resulting in the reduction of the role of the more rough outer interface. The larger roughness of the outer interface seems to be natural for the quantum well heterostructures studied because lattice mismatch leads to a strain of  $\text{In}_x\text{Ga}_{1-x}\text{As}$  layer and corrugation of outer interface. Analogous results were obtained in Ref. 3 for silicon MOSFET.

## B. Effect of nanoclusters on the weak localization

Now let us consider the effect of in-plane magnetic field on the negative magnetoresistance for structure H5610 with nanoclusters. The  $[\sigma(B_\perp, B_\parallel) - \sigma(0, B_\parallel)]$ -versus- $B_\perp$  plot for structure H5610#2 is presented in Fig.4. As seen from Fig.4(a) the negative magnetoresistance measured at  $B_\parallel = 0$  is perfectly described by Eq. (1). If one tries to fit by Eq. (1) the data measured at  $B_\parallel \neq 0$  one finds that the fitting parameters strongly depend on the fitting interval. For instance, the prefactor  $\alpha$  strongly decreases from  $\alpha = 2.2$  to  $\alpha = 1.4$  when the fitting interval of  $B$  is expanded from  $0 - 0.1$  to  $0 - 0.2$  [see Fig.4(a)]. Moreover, the significantly higher than unity value of the prefactor is unreasonable for single quantum well structure with one occupied subband. All this points to the fact that Eq. (1) rather poorly describes the experimental data for structure H5610. We believe that such a behavior is sequence of a long-range correlated roughness which is caused by nanoclusters. The presence of nanoclusters in this structure leads to smooth random deviation in position of an electron in growth direction when it moves over the quantum well [see inset in Fig. 4(a)]. Influence of in-plane magnetic field on the shape of magnetoresistance curve in perpendicular field for

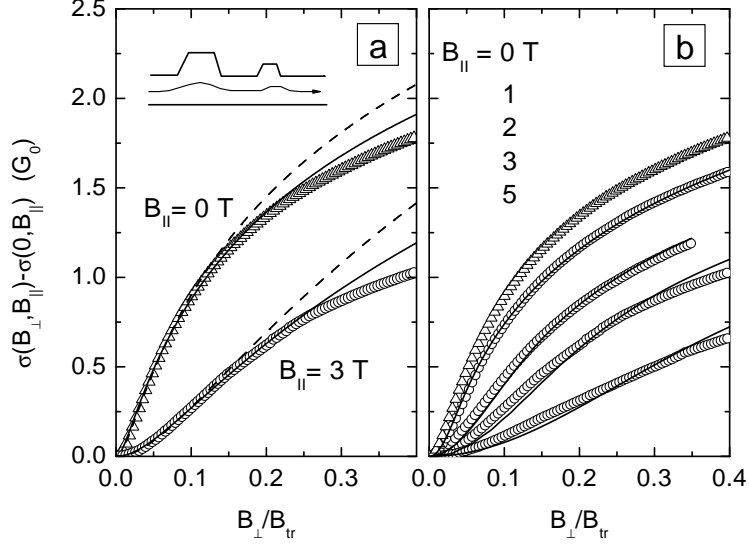


FIG. 4: The  $[\sigma(B_{\perp}, B_{\parallel}) - \sigma(0, B_{\parallel})]$ -versus- $B_{\perp}$  dependences for structure H5610#2 taken at  $T = 1.45$  K and  $V_g = -2.5$  V. Symbols are the experimental data. Curves in (a) are the best fit by Eq. (1) with parameters:  $B_{\parallel} = 0$  –  $\alpha = 1.0$ ,  $\tau_{\varphi} = 1.2 \times 10^{-11}$  s (dashed line) and  $\alpha = 0.9$ ,  $\tau_{\varphi} = 1.45 \times 10^{-11}$  s (solid line);  $B_{\parallel} = 3$  T –  $\alpha = 2.2$ ,  $\tau_{\varphi} = 2.3 \times 10^{-12}$  s (dashed line) and  $\alpha = 1.4$ ,  $\tau_{\varphi} = 2.9 \times 10^{-12}$  s (solid line). Dashed and solid curves correspond to the fitting interval  $B = (0-0.1)B_{tr}$  and  $B = (0-0.2)B_{tr}$ , respectively. Curves in (b) are the best fit by Eq. (5) in which the Gaussian distribution and experimental curve  $\sigma(B_{\perp}, 0)$  are used for  $F(\beta)$  and  $\delta\sigma(B_{\perp} + \beta B_{\parallel}, \tau_{\varphi})$ , respectively. The values of fitting parameter  $\Delta_{\beta}$  sequence from  $B_{\parallel} = 1$  T to  $B_{\parallel} = 5$  T are the in following: 0.34; 0.41; 0.47; 0.52 degrees. Inset in (a) is a schematic representation of electron motion along the quantum well with one rough side.

the case  $l_{\varphi} > L > l_p$  was theoretically studied in Ref. 4. However the final expressions are very complicate and cumbersome to compare them with the experimental curves directly.

Another limiting case  $L > l_{\varphi}$  is very simple and transparent from the physical point of view. In this case one can consider that all the actual closed paths lie on the flat elements of size larger than  $l_{\varphi}$ , which are inclined from ideal 2D plane through small random angles  $\beta$ . This means that the resulting magnetoresistance is a sum of the contributions of these deflected elements. The contribution of each element is  $\delta\sigma(B_n, \tau_{\varphi}) = \delta\sigma(B_{\perp} + \beta B_{\parallel}, \tau_{\varphi})$ , where  $B_n$  is projection of the total magnetic field onto the normal to the element plane.

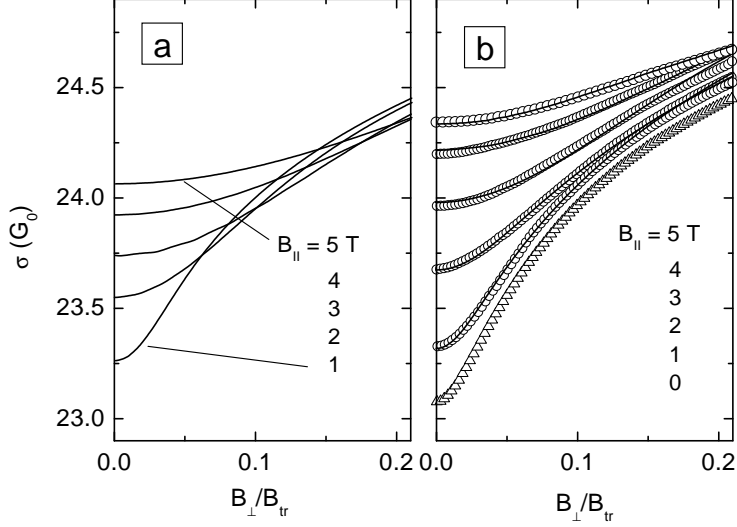


FIG. 5: (a) The  $B_{\perp}$ -dependences of absolute values of the conductivity taken at different in-plane magnetic field. Lines in (a) are the just the same as in Fig. 4(b) but plotted without subtraction of the value of  $\sigma(0, B_{\parallel})$ . Symbols in (b) are the experimental data, lines are obtained taking into account both long- and short-range correlated roughness. The fitting parameters as a functions of in-plane magnetic field are shown in Fig. 6.

Then, the total magnetic field dependence of the conductivity can be written as

$$\sigma(B_{\perp}, B_{\parallel}, \tau_{\varphi}) = \int d\beta F(\beta) \delta\sigma(B_{\perp} + \beta B_{\parallel}, \tau_{\varphi}), \quad (5)$$

where  $F(\beta)$  is the distribution function of the deflection angles. To compare this expression with experimental data one needs to specify the functions in the right-hand side of Eq. (5). We have used the Gaussian distribution for  $F(\beta)$  with root-mean square  $\Delta_{\beta}$ . The experimental  $\sigma$ -versus- $B_{\perp}$  curve measured at  $B_{\parallel} = 0$  has been used as  $\delta\sigma(B_{\perp} + \beta B_{\parallel}, \tau_{\varphi})$ . The result of the fitting procedure for  $\sigma(B_{\perp}, B_{\parallel}) - \sigma(0, B_{\parallel})$  with one fitting parameter  $\Delta_{\beta}$  is shown in Fig. 4(b). One can see that this simple model perfectly describes the shape of the experimental magnetoresistance curve in the presence of in-plane magnetic field up to  $B_{\parallel} = 2$  T and the parameter  $\Delta_{\beta}$  found from the fit is really small in magnitude:  $\Delta_{\beta} \simeq 0.3^{\circ} - 0.4^{\circ}$ . A noticeable discrepancy between this model and experimental observations is evident at higher magnetic field,  $B \gtrsim 3$  T, the parameter  $\Delta_{\beta}$  sufficiently increases with  $B_{\parallel}$  increase [see Fig. 6(a)]. To our opinion, the situation when  $\Delta_{\beta}$  is independent of in-plane magnetic field seems more natural.

Such a discrepancy between this model and experimental observations evident at  $B_{\parallel} \gtrsim$

3 T can be understood if one supposes a simultaneous existence of short- and long-range correlated roughness in the structure H5610. As shown above the short-range correlated roughness results effectively in lowering of  $\tau_\varphi$  in in-plane magnetic field. Thus, it becomes meaningless to use the experimental  $\sigma$ -versus- $B_\perp$  curve measured at  $B_\parallel = 0$  in right-hand side of Eq. (5) when  $B_\parallel$  is rather high.

The presence of short-range correlated roughness in structure H5610 is more pronounced when considering the effect of in-plane magnetic field on the absolute value of the conductivity. Figure 5(a) shows the curves shown in Fig. 4(b) but plotted without subtraction of  $\sigma(0, B_\parallel)$ . Comparing this figure with Fig. 5(b), in which the experimental results are presented, one can see that the model taking into consideration only the long-range correlated roughness does not describe the behavior of absolute value of  $\sigma$  in in-plane magnetic field. It is most conspicuous at  $B_\perp/B_{tr} \gtrsim 0.1$ , where the experimental  $\sigma$ -versus- $B_\perp$  plots are shifted up with  $B_\parallel$ -increase whereas the calculated curves tend to merge together. It is natural to suggest that the shift of experimental curves is a result of the influence of short range correlated roughness which leads to decrease of  $\tau_\varphi$  and, thus, to increase of the conductivity with increasing of in-plane magnetic field when the perpendicular field is fixed.

To take into account coexistence of both long- and short-range correlated roughness in our model, we have used the quantity  $\sigma(B_\perp = 0, B_\parallel = 0) + \alpha G_0 H(B, \tau_\varphi)$  as  $\delta\sigma(B_\perp + \beta B_\parallel, \tau_\varphi)$  in Eq. (5), where  $\sigma(B_\perp = 0, B_\parallel = 0)$  is measured experimentally. Thus, we can manipulate by three fitting parameters  $\alpha$ ,  $\tau_\varphi$ , and  $\Delta_\beta$  to describe quantitatively the experimental results for structure H5610. Figure 5(b) illustrates excellent agreement between experimental results and the model taking into account both types of roughness.

Let us now consider whether the fitting parameters are reasonable. First of all, the value of the prefactor is about 0.8 – 0.9 that agrees with sufficiently large  $\tau_\varphi$  to  $\tau$  ratio at any  $B_\parallel$ :  $\tau_\varphi/\tau \simeq 100 - 200$ . Second, the parameter  $\Delta_\beta$  does not practically depend on  $B_\parallel$  and is close to that obtained at  $B_\parallel < 3$  T without taking into account the short-range correlated roughness [see Fig. 6(a)]. Thus, the value of  $\Delta_\beta$  characterizing the long-range correlated roughness can be estimated at  $0.35^\circ$ . Finally, the fitting parameter  $1/\tau_\varphi^*$  exhibits quadratical increase when  $B_\parallel$  increases [see Fig. 6(b)], that allows us to estimate the scale of the short-range correlated roughness using Eqs. (2) and (3). The value of  $\Delta^2 L$  in structure H5610 with nanoclusters occurs to be about  $1.2 \text{ nm}^3$  that is less than that for structure 3512. Such an analysis carried out for other gate voltages shows that the parameter  $\Delta_\beta$  is

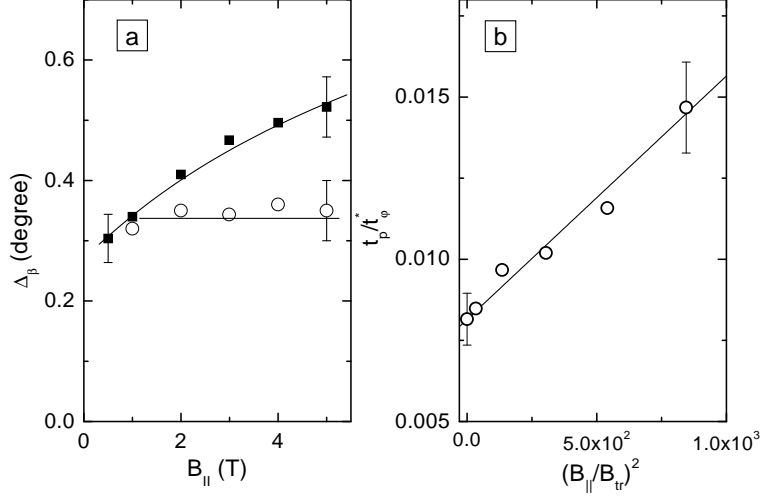


FIG. 6: The fitting parameters  $\Delta_\beta$  (a) and  $\Delta^2 L$  (b) corresponding to solid lines in Fig. 5(b) as functions of in-plane magnetic field. Solid symbols correspond to the long-range roughness model, open symbols are obtained when both short- and long-range roughness are taken into consideration. Lines in (a) are provided as a guide to the eye, line in (b) is calculated from Eqs. (2) and (3) using  $\Delta^2 L = 1.4 \text{ nm}^3$  and experimental values  $l_p = 44 \text{ nm}$  and  $\tau_p/\tau_\phi = 8.15 \times 10^{-3}$ .

independent of electron density within experimental error and, thus, is about  $0.35^\circ$  and the parameter  $\Delta^2 L$  increases from approximately 1 to  $1.8 \text{ nm}^3$  when the electron density varies from  $0.59 \times 10^{12}$  to  $0.91 \times 10^{12} \text{ cm}^{-2}$  [see Fig. 3(c)]. As for structure 3512 (see Section III A), we believe that such a behavior of  $\Delta^2 L$  is a result of the shift of the wave function to inner smooth interface of the quantum well that in its turn leads to reduction of the role of outer rough interface.

Thus, for the 2D structure with nanoclusters we can adequately describe the influence of in-plane magnetic field on weak localization combining two limiting theoretical models corresponding to short- and long-range correlated roughness.

### C. Results of AFM-studies

To assure that the structure H5610 distinguishes from the structure 3512 by the presence of long-range correlated roughness and to estimate its parameters, we have attempted to measure the profile of the quantum well surface. For this purpose the cap layer was removed using the selective etching.<sup>9</sup> After that the surface was scanned by Atomic Force Microscope

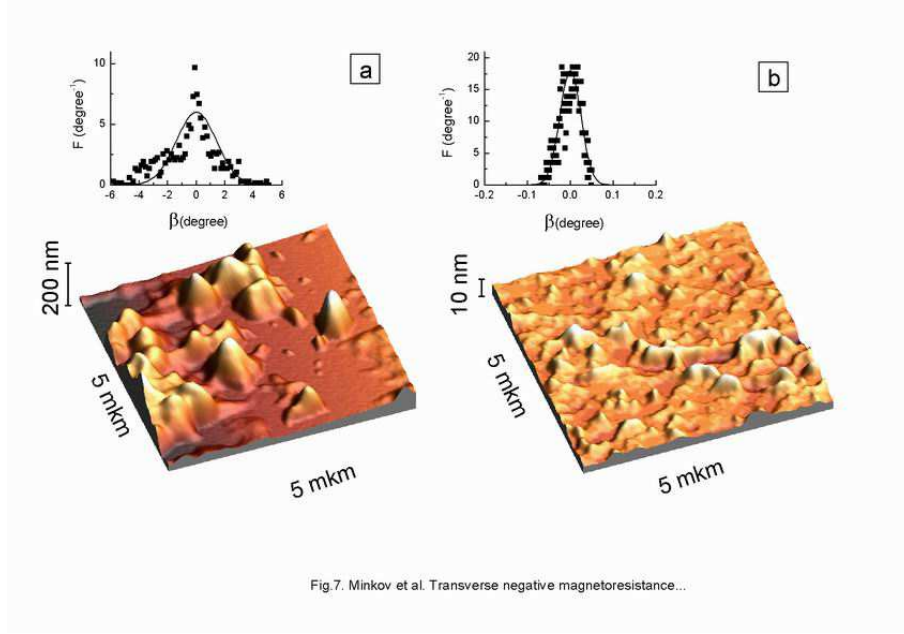


FIG. 7: The AFM images for structure H5610 (a) and 3512 (b) obtained after removing of the cap layer. Insets show the angle distribution function  $F(\beta)$  obtained for  $\mathcal{L} = 2l_\varphi$  (see text) The values of  $l_\varphi$  at  $T = 1.5K$  are 490 nm and 870 nm for structures H5610 and 3512, respectively.

(AFM) using TopoMetrix Accurex TMX-2100 ambient air AFM in Contact Mode.  $\text{Si}_3\text{N}_4$  pyramidal probes were employed. The AFM-images for both structures are shown in Fig. 7. It is clearly seen that the scales of surface roughness are drastically different. In order to get the quantitative information corresponding to our experiments, we have processed the images.

Let us firstly consider the long-range roughness. In accord with the model used for interpretation of the results for structure H5610 the surfaces presented in Fig. 7 were approximated by set of the flat squares of size  $\mathcal{L} > l_\varphi$ , then the angle distribution function  $F(\beta)$  entering in Eq. (5) was found. This function is presented in insets in Fig. 7 for both structures. It has been approximated by the Gaussian distribution and the dispersion  $\Delta_\beta$  has been found. The value of  $\Delta_\beta$  obtained for  $\mathcal{L} = 2l_\varphi$  and  $\mathcal{L} = 3l_\varphi$  was close and differed by 30%.

For structure H5610 the value of  $\Delta_\beta$  is about  $2^\circ$  that is five-six times larger than the dispersion obtained from the weak localization measurements [see Fig. 6]. The reason for such a discrepancy is qualitatively clear. In reality, an electron moves not over the surface, it moves in the quantum well laying under the surface. Therefore, the deviations of electron in

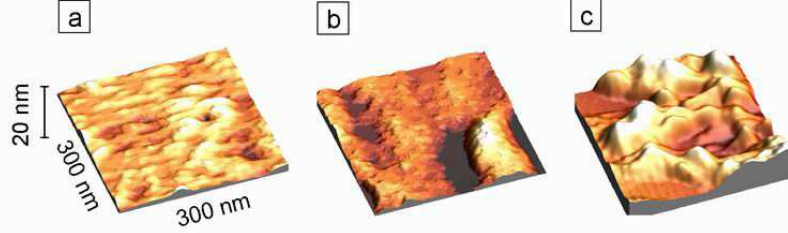


FIG. 8: The AFM images for structure 3512 (a) and H5610 (b,c), scanned area is  $300 \times 300$  nm.

$z$ -direction are smaller than the roughness magnitude. Thus, we consider the results of weak localization and AFM experiments being in a satisfactory agreement for structure H5610.

For structure 3512, the dispersion is about  $0.035^\circ$ , i.e., the long range correlated roughness is practically absent. This fact agrees with the experimental result that only the short range correlated roughness reveals itself in weak localization in the presence of in-plane magnetic field.

To estimate the parameter  $\Delta^2 L$  responsible for the influence of the short-range correlations on the weak localization, the surfaces have been scanned with the higher resolution (Fig. 8). The mean peak spacing for structure 3512 found from AFM-image given in Fig. 8(a) is 65 nm, that is really less than mean free path ( $l_p = 210$  nm for  $V_g = 0$ ). So the use of the short-range correlated roughness model is justified. The value of  $\Delta$  found as a root-mean square deviation in  $z$ -direction is about 0.35 nm. So, we obtain from independent AFM-measurements the parameter  $\Delta^2 L \simeq 8$  nm<sup>3</sup> which is close to that obtained from weak-localization experiment [see Fig. 3(c)].

It is more difficult to carry out the analogous estimation for structure H5610. First, the flat and hilly areas look differently at this resolution [see Figs. 8(b) and 8(c)]. Second, the peak spacing distribution is very wide and has no maximum. Nevertheless we try to estimate  $\Delta$  using  $l_p/2$  as  $L$ . The value of  $\Delta$  found for the flat and hilly areas appears to be different:

0.2 and 0.6 nm, respectively. Therefore, the value of parameter  $\Delta^2 L$  for these areas are significantly different 1.6 nm<sup>3</sup> and 14 nm<sup>3</sup> (we used here  $l_p = 80$  nm that corresponded  $V_g = 0$ ). Recall that  $\Delta^2 L$  obtained from the weak localization experiments is  $(2 \pm 0.5)$  nm [see Fig. 3(c)]. Taking into account the large scatter of AFM results, we consider such an agreement as satisfactory.

#### IV. CONCLUSION

We have experimentally studied the effects of in-plane magnetic field on the interference induced negative magnetoresistance in perpendicular magnetic field for different types of quantum well heterostructures. It has been shown that the effects significantly depend on the relationship between mean free path and in-plane size of the roughness. The analysis of the shape of the negative magnetoresistance at in-plane magnetic field gives possibility to recognize the characteristic in-plane scale of the roughness and estimate its parameters. The results of weak localization studies have been found in a good agreement with evidence from AFM measurements.

#### Acknowledgments

This work was supported in part by the RFBR through Grants No. 01-02-17003, No. 01-02-16441, No. 03-02-16150, and No. 03-02-06025, the CRDF through Grants No. REC-001 and No. REC-005, the Program *University of Russia* through Grant No. UR.06.01.002, and the Russian Program *Physics of Solid State Nanostructures*.

---

\* Electronic address: Grigori.Minkov@usu.ru

<sup>1</sup> Julia S. Meyer, Alexander Altland, and B. L. Altshuler, Phys. Rev. Lett. **89**, 206601 (2002).

<sup>2</sup> A. G. Mal'shukov, K. A. Chao, and M. Willander, Phys. Rev. B **56**, 6436 (1997).

<sup>3</sup> P. M. Mensz and R. G. Wheeler, Phys. Rev. B **35**, 2844 (1987).

<sup>4</sup> H. Mathur and Harold U. Baranger, Phys. Rev. B **64**, 235325 (2001).

<sup>5</sup> G. M. Minkov, A. V. Germanenko, O. E. Rut, A. A. Sherstobitov, B. N. Zvonkov, E. A. Uskova, and A. A. Birukov, Phys. Rev. B **64**, 193309 (2001).



- <sup>6</sup> G. M. Minkov, O. E. Rut, A. V. Germanenko, A. A. Sherstobitov, B. N. Zvonkov, E. A. Uskova, and A. A. Birukov, Phys. Rev. B **65**, 235322 (2002).
- <sup>7</sup> S. Hikami, A. Larkin and Y. Nagaoka, Prog. Theor. Phys. **63**, 707 (1980).
- <sup>8</sup> A. G. Malshukov, V. A. Frolov and K. A. Chao, Phys. Rev. B **59**, 5702 (1999).
- <sup>9</sup> R. Retting, W. Stolz. Physica E. **2**, 1998 (1998).